Applied Catalysis B: Environmental 90 (2009) 699–704

Contents lists available at ScienceDirect

Applied Catalysis B: Environmental

journal homepage: www.elsevier.com/locate/apcatb

Paper-structured fiber composites impregnated with platinum nanoparticles synthesized on a carbon fiber matrix for catalytic reduction of nitrogen oxides

Hirotaka Koga [a], Yuuka Umemura [a], Hirotake Ishihara [a], Takuya Kitaoka [a,*], Akihiko Tomoda [b], Ryo Suzuki [b], Hiroyuki Wariishi [a]

[a] Department of Forest and Forest Products Sciences, Graduate School of Bioresource and Bioenvironmental Sciences, Kyushu University, 6-10-1 Hakozaki, Higashi-ku, Fukuoka 812-8581, Japan
[b] R&D Division, F.C.C. Co. Ltd., Kita-ku, Hamamatsu, Shizuoka 431-1304, Japan

ARTICLE INFO

Article history:
Received 28 December 2008
Received in revised form 31 March 2009
Accepted 5 May 2009
Available online 9 May 2009

Keywords:
Carbon fiber
Platinum nanoparticles
Paper-structured catalyst
Nitrogen oxides
Catalytic gas purification

ABSTRACT

Platinum nanoparticles (PtNPs) were synthesized on surface-activated carbon fibers with high thermal conductivity, and paper-structured composites were fabricated by a papermaking technique, using the PtNPs-supported carbon fibers and ceramic fibers as matrix materials. As-prepared materials, denoted paper-structured PtNPs catalyst, possessed a unique porous microstructure derived from entangled inorganic fiber networks on which PtNPs were well dispersed. In catalytic reduction of nitrogen oxides (NO_X) in the presence of methane (CH_4), both of which are model exhaust gas components of combustion engines, paper-structured PtNPs catalyst demonstrated excellent NO_X and CH_4 removal efficiency and rapid thermal responsiveness by comparison with the PtNPs-supported carbon fibers, commercial Pt catalyst powders and a monolithic Pt-loaded honeycomb. These features of the new catalyst material are thought to arise from synergistic effects of the highly active PtNPs in association with the unique paper-like microstructure, in promoting effective transfer of heat and reactants to the active sites of the Pt nanocatalysts. The paper-structured PtNPs catalyst with paper-like practical utility is expected to be a promising catalytic material for efficient NO_X gas purification.

© 2009 Elsevier B.V. All rights reserved.

1. Introduction

In recent years, air pollution has been exacerbated by an increasing volume of exhaust gases generated by plant boilers and vehicles with internal combustion engines [1,2]. In particular, automobile exhaust gases such as nitrogen oxides (NO_X), carbon monoxide (CO) and hydrocarbons (HC) are considered to be the major cause of global air pollution [2,3]. Efficient purification of such exhaust gases is thus essential for environmental cleanup and protection. Exhaust gas purification is generally carried out using noble metal catalysts such as platinum (Pt), rhodium and palladium [3–9]. However, these noble metals are limited resources and reduction of their usage has become important for wider applications [10].

A variety of catalysts for gas purification have been developed with the aim of achieving low cost, energy conservation and high performance with small amounts of noble metals [11,12]. Metal nanoparticles (NPs) have attracted much attention as highly active catalysts due to their large surface area to volume ratio and numerous catalytic sites [13–15]. However, metal NPs easily aggregate to minimize their large surface area and eventually yield bulk-like properties, leading to marked reduction of catalytic activity [16]. To overcome undesirable aggregation, catalyst NPs are generally immobilized on supports such as alumina [17], titania [18] and zeolite [19].

At the present time, functional design of catalyst support and matrix is being intensively investigated for practical applications [20–22]. Catalyst NPs are generally supported on fine particles, but such powder form catalysts are difficult to handle in practical use; thus they are molded into various forms such as pellets and beads. However, their catalytic performance then markedly decreases compared with that of the original materials [23]. Furthermore, random packing of solid catalysts into reactors inevitably results in a high pressure drop and fluid bypassing, and inefficiency of the overall catalytic process. Recently monolithic ceramic supports with honeycomb structure have become popular due to their low pressure drop and large relative surface area, especially as NO_X purification catalysts [24,25]. However, honeycomb-structured catalysts in general have the disadvantages of heaviness, poor lateral diffusion of reactant gases and low thermal conductivity [26]. There is, consequently, a strong demand for new types of catalytic materials for efficient gas purification.

In our previous studies, copper/zinc oxide (Cu/ZnO) catalyst powders were successfully supported on a microstructured paper

* Corresponding author. Tel.: +81 92 642 2993; fax: +81 92 642 2993.
E-mail address: tkitaoka@agr.kyushu-u.ac.jp (T. Kitaoka).

0926-3373/$ – see front matter © 2009 Elsevier B.V. All rights reserved.
doi:10.1016/j.apcatb.2009.05.002

matrix with layered ceramic fiber networks by use of a papermaking technique [27–31]. As-prepared materials, denoted paper-structured catalyst, were lightweight, flexible, easy to handle, and showed high catalytic performance compared with commercial catalysts, for methanol reforming to produce hydrogen for fuel cell applications. It was found that the unique fiber network microstructure with connected spaces may provide a favorable reaction environment to promote desirable gas diffusion within the catalyst layer. In a recent study, direct *in situ* synthesis of CuNPs on ZnO whiskers embedded in a paper-like matrix was achieved; the CuNPs@ZnO paper composite demonstrated extremely high catalytic performance for hydrogen production [32].

In the present study, a novel paper-structured catalyst with PtNPs supported on carbon fibers was prepared by combination of these approaches, and applied to catalytic reduction of NO as a model automobile exhaust gas. Synthesis of PtNPs was accomplished on a carbon fiber matrix that was pre-treated with nitric acid to activate the surface. Paper-like catalyst composites impregnated with PtNPs-supported carbon fibers with high thermal conductivity were fabricated with ceramic fibers as another fiber matrix, using our established papermaking technique. The catalytic performance of paper-structured PtNPs catalyst was compared with the performance of commercial Pt/aluminum oxide (Al_2O_3) catalyst powders and monolithic Pt-loaded honeycomb, in catalytic reduction of NO in the presence of methane (CH_4), for exhaust gas purification.

2. Experimental

2.1. Materials

Hexachloroplatinic acid (H_2PtCl_6, Pt content 198.75 g L^{-1}), commercial Pt/Al_2O_3 catalyst powder (Pt content 1 wt.%) and a monolithic honeycomb-structured cordierite catalyst (400 channels per square inch, 5.6×10^3 mm^3 per piece, Pt content 750 g m^{-3}) were purchased from Tanaka Kikinzoku Kogyo Co., Ltd. Carbon fibers (with thermal conductivity 515 W m^{-1} K^{-1}; Mitsubishi Kagaku Sanshi Co., Ltd.) and ceramic fibers (Ibiwool, Ibiden Co., Ltd.) were washed with water and cut to average length 0.5 mm with a blender. Pulp fibers as a temporary supporting matrix in the papermaking process were obtained by refining commercial bleached hardwood kraft pulp to average length about 0.5 mm using a standard beater. Two types of flocculants were used for paper fabrication, namely cationic polydiallyldimethylammonium chloride (PDADMAC; molecular weight ca. 3×10^5 g mol^{-1}, charge density 5.5 meq g^{-1}; Aldrich Co., Ltd.) and anionic polyacrylamide (A-PAM, HH-351; molecular weight ca. 4×10^6 g mol^{-1}, charge density 0.64 meq g^{-1}; Kurita Co., Ltd.). Alumina sol (Snowtex 520, Nissan Chemicals Co., Ltd.) was used as a binder to improve the physical strength of the paper composites after calcination.

2.2. Synthesis of PtNPs on carbon fibers

Synthesis of PtNPs on carbon fibers was carried out in part according to a previous report [33]. Carbon fibers (5.0 g) were soaked in 35% nitric acid solution (14.3 mL) at room temperature, followed by stirring for 2 h, filtration, thorough washing with distilled water and drying at 105 °C for 24 h. The carbon fibers obtained were suspended in an aqueous solution of H_2PtCl_6 (6.4 mM), and the mixture was stirred at room temperature for 12 h, followed by evaporation at 150 °C to complete dryness. The carbon fibers treated with H_2PtCl_6 solution were put into a stainless steel cylinder and reduced with a gaseous mixture of hydrogen (25 standard cubic centimeters per minute (SCCM)) and nitrogen (100 SCCM) at 55 °C for 2 h.

2.2.1. Preparation of paper-structured PtNPs catalysts by a papermaking technique

The preparation details of paper composites using organic and inorganic fibers, through a dual polyelectrolyte retention system, have been described in our previous reports [27–32]. In summary, a ceramic fiber/water suspension (1.0%, w/v) containing a designated amount of PtNPs-supported carbon fibers was mixed with PDADMAC (0.5 wt.% per solids), alumina sol binder and A-PAM (0.5 wt.% per total solids), in that order. Finally, a pulp fiber suspension was poured into the mixture, followed by dewatering using a 200-mesh wire and subsequent pressing at 350 kPa for 3 min. The wet handsheets were dried in an oven at 105 °C for 1 h. The resulting paper composite consisted of PtNPs-supported carbon fibers (2.75 g), ceramic fibers (2.25 g), alumina sol (0.5 g) and pulp fibers (1.0 g). The as prepared PtNPs-supported carbon fiber-containing paper-structured catalyst composites were calcined at 500 °C for 30 min to remove organic pulp fibers and to improve the physical strength by sintering of the alumina sol binder.

2.3. Catalytic performance test

Seven circular pieces of paper-structured PtNPs catalyst composite, each with area 800 mm^2 and thickness 1.0 mm, were vertically stacked (5.6×10^3 mm^3) in a cylindrical reactor of stainless steel, so that they were in contact with the inner wall of the reactor. As-prepared PtNPs-supported carbon fibers and commercial Pt/Al_2O_3 powders were mixed with designated fiber components to adjust the total occupied volume to 5.6×10^3 mm^3, and set inside the reactor. A monolithic honeycomb-structured cordierite (5.6×10^3 mm^3) was placed as is inside the reactor. In each case, the amount of Pt catalyst was maintained at 4.2 mg per test sample. The flows of gaseous reactants were regulated by mass flow controllers (Model 3660 or 3200 SR Series, Kofloc Co., Ltd.). A gas mixture composed of NO (400 ppm), CH_4 (2440 ppm), O_2 (0.46%) and He (balance) was heated to 170 °C and continuously passed through the packed catalyst samples at a constant flow rate of 5.0×10^5 mm^3 min^{-1} at atmospheric pressure. The internal temperature of the reactor was controlled by a continuous heat supply system comprising a mantle heater and a thermocouple inserted in the middle layer of the catalyst samples. The external temperature of the reactor was simultaneously monitored using a thermocouple inserted in the mantle heater. In the steady state, the gas composition during the catalytic reaction was monitored online using an NO_X analyzer (NOA-7000, Shimadzu Co., Ltd.) and a gas chromatograph (GC, GC-8A, Shimadzu Co., Ltd.) with thermal conductivity detector and a Porapak-Q column (3 mm × 1 m, Shinwa Chemical Industries, Ltd.). To elucidate the thermal responsiveness of catalyst samples, catalytic performance tests at elevated temperatures were conducted at a heating rate of 2 °C min^{-1}.

2.4. Analyses

Transmission electron microscopy (TEM) was carried out using a JEM1010 instrument (JEOL, Ltd.) at 80 kV accelerating voltage. The chemical states of component elements were analyzed using X-ray photoelectron spectroscopy (XPS, AXIS-HSi, Shimadzu/Kratos, Ltd.) with a monochromatic AlKα X-ray source (1486.6 eV) operating at 15 kV and 10 mA, and analyzing chamber pressure below 5×10^{-7} Pa. X-ray diffractometry (XRD) studies were conducted using an XD-D1 X-ray diffractometer (Shimadzu, Ltd.) with Ni-filtered CuKα radiation (λ = 1.5418 Å) at 30 kV and 40 mA. The Scherrer formula was used to calculate the Pt crystallite size on the basis of the full width at half maximum of the Pt(1 1 1) reflection [34]. The Pt contents of PtNPs-supported carbon fibers

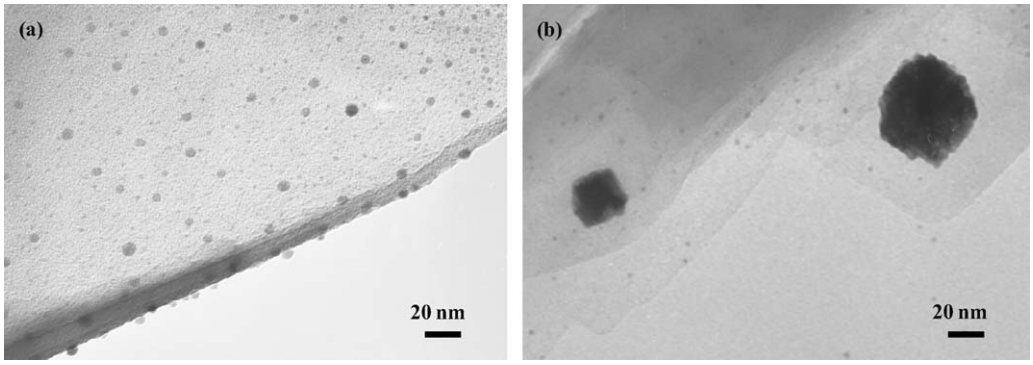

Fig. 1. TEM images of PtNPs-supported carbon fiber with (a) acid pre-treatment and (b) Pt-precipitated carbon fiber without acid pre-treatment.

and paper-structured PtNPs catalyst were determined by atomic absorption spectrophotometry using a Shimadzu AA-6600F instrument: the concentration of Pt ions eluted from the samples with a 3:1 mixture of 36% hydrochloric acid and 69% nitric acid was measured. The fiber-network microstructure of the paper-structured catalyst was visualized by confocal laser scanning microscopy (CLSM; ECLIPSE TE2000-U, Nikon Co., Ltd.) with a solid-state laser at 488 nm. Mercury intrusion analysis was carried out using a Poremaster 33P (Yuasa Ionics, Ltd.) to evaluate pore diameter and porosity of the catalyst samples.

3. Results and discussion

3.1. Synthesis and characterization of PtNPs on carbon fibers

Efficient immobilization of metal NPs is the focus of attention for practical applications of NP-form catalysts. Surface activation of a carbon matrix by acid treatment has been reported recently for the introduction of oxygen-anchoring groups, to facilitate adsorption of metal ions [33,35]. In the present work, this approach was applied to carbon fibers as a support matrix for Pt species. Fig. 1 displays TEM images of Pt-synthesized carbon fibers with and without acid pre-treatment. In the case of surface-activated carbon fibers, a large number of PtNPs with size less than 10 nm were uniformly dispersed on the fiber surfaces (Fig. 1a). By contrast, relatively massive Pt aggregates adhered to the surface of carbon fibers that had not been subjected to the pre-treatment with acid (Fig. 1b). Although both acid-treated and untreated fibers were subjected to reduction by hydrogen flow under the same conditions, the surface activation of carbon fibers led to distinctly smaller Pt-derived spots. Furthermore, the Pt loadings of the pre-treated and the untreated fibers were about 5.4 and 3.8 mg g^{-1} of carbon fiber, respectively, from atomic absorption analysis. It seems, then, that the acid pre-treatment was an essential step in the process for effective PtNPs synthesis on the carbon fibers. The XPS analysis showed that the atomic ratio of oxygen (O1s: 532 eV) to carbon (C1s: 285 eV) increased from 0.036 to 0.051 by acid pre-treatment, suggesting that oxygen-anchoring groups were introduced by the acid pre-treatment on the surfaces of carbon fibers, as reported in previous papers [36–38]. The oxygen-anchoring groups facilitated effective Pt adsorption, leading to highly dispersed PtNPs on the pre-treated carbon fibers. Atomic absorption analysis indicated that about 90% of the added Pt species was successfully supported on the carbon fibers.

The chemical states of the component elements were analyzed by XPS. Fig. 2 shows narrow scans of Pt4d and Cl2s for the surfaces of carbon fibers treated with H_2PtCl_6, before and after hydrogen reduction. As-dried Pt-carbon fibers displayed a Pt4d peak at ca. 317 eV, corresponding to an ionic Pt species [39], and a well-defined Cl2 s peak at ca. 270 eV, which is assigned to Cl^- ions [40]. After hydrogen reduction, a shift of the Pt4d peak from 317 to about 315 eV was observed, and the Cl2 s peak disappeared, indicating that the Pt species was fully reduced from ionic Pt to metallic Pt(0). Both commercial Pt/Al_2O_3 powders and honeycomb monolithic catalyst had metallic Pt(0) components (see supplementary data, Fig. S1). Fig. 3 shows XRD patterns of the original carbon fibers and PtNPs-supported carbon fibers. The original fibers showed reflections typical of graphite crystals, and the PtNPs-supported carbon fibers displayed four new peaks at (2θ) 40, 46, 68 and 81° that are attributed to Pt crystals [41], indicating successful formation of Pt nanocrystals (with crystallite size ca. 7.6 nm). From the TEM observation of PtNPs-supported carbon

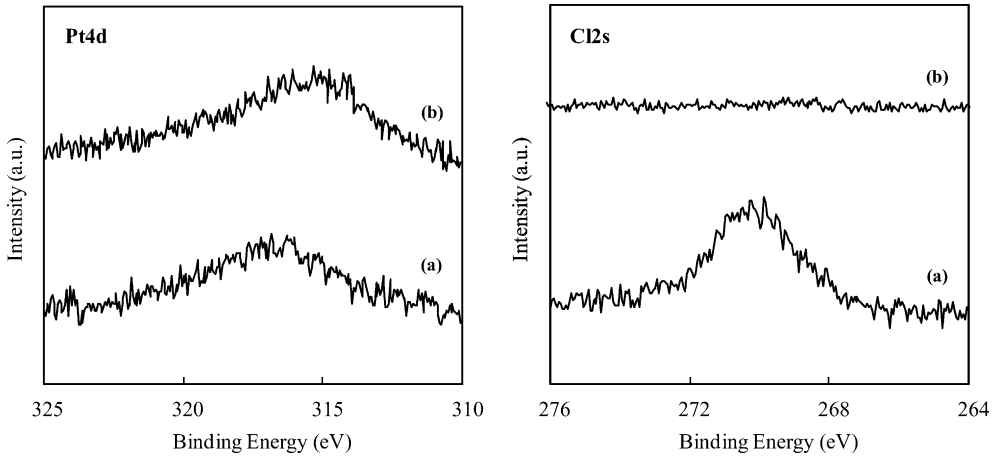

Fig. 2. XPS profiles of carbon fibers treated with H_2PtCl_6: (a) as-dried and (b) reduced.

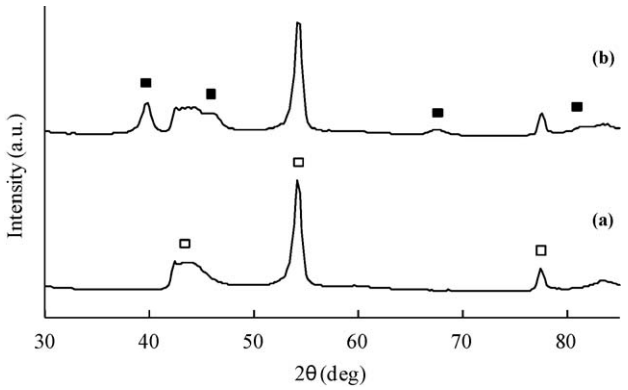

Fig. 3. XRD patterns of (a) carbon fibers and (b) PtNPs-supported carbon fibers; (□) carbon (graphite) and (■) Pt.

fibers (Fig. 1a), it seems likely that the PtNPs were supported on the carbon fiber matrix as single crystals. The Pt crystallite size of commercial Pt/Al_2O_3 powders was ca. 7.8 nm, being equivalent to that of PtNPs on the carbon fibers (see supplementary data, Fig. S2a); however, the accurate Pt crystallite size of commercial honeycomb catalyst could not be estimated due to the peak overlapping of Pt and cordierite components (Fig. S2b).

3.2. Fiber-network microstructure of paper-structured PtNPs catalyst

In our previous studies, paper-structured matrices composed of inorganic fibers and catalyst powders were prepared using a high-speed, low-cost papermaking technique [27–31]. In the present study, highly active PtNPs supported on carbon fibers were successfully fabricated into paper composites by combined use of PtNPs-supported carbon fibers and ceramic fibers as a matrix material. Fig. 4 displays optical images of paper-structured PtNPs catalyst and commercial honeycomb catalyst as a reference material. The paper-structured PtNPs catalyst was strengthened by sintering of an alumina sol binder (500 °C, 30 min), while almost no combustion of carbon fibers was found at a temperature below 600 °C (see supplementary data, Fig. S3). The resulting paper-structured PtNPs catalyst with the appearance of flexible cardboard was easy to handle. Fig. 5 shows 2D reflected and 3D fluorescent CLSM images of the fiber-network microstructure of the paper-structured catalyst. The 2D reflected image (Fig. 5a) shows carbon and ceramic fibers entangled with each other. Fluorescent imaging distinguished carbon (yellow or red in color) and ceramic fibers (blue) by detecting the difference in inherent self-fluorescence of inorganic components, as shown in Fig. 5b. The CLSM image capturing system, whereby the focal planes are successively staggered every 0.5 μm in a vertical (height) direction, was used to build the 3D image inside a paper-structured

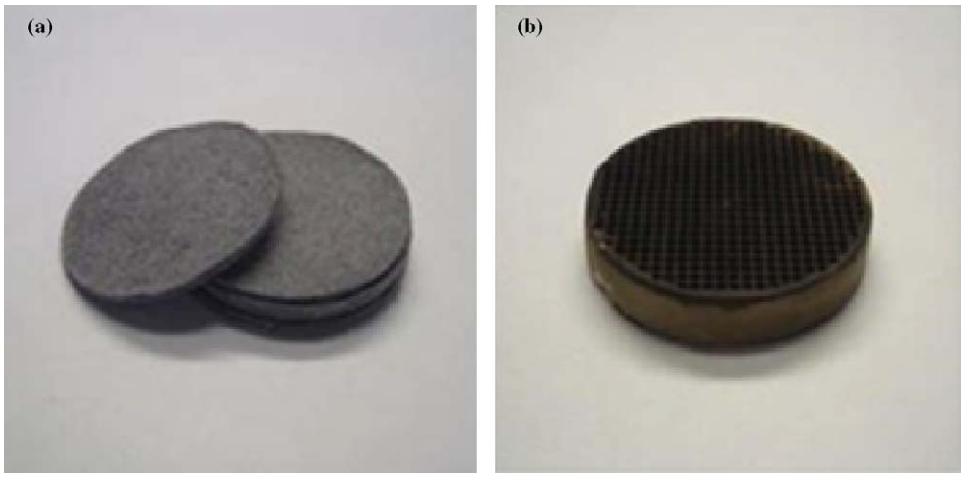

Fig. 4. Optical images of (a) paper-structured PtNPs catalyst, and (b) commercial honeycomb monolithic catalyst. Each sample is 32 mm in diameter.

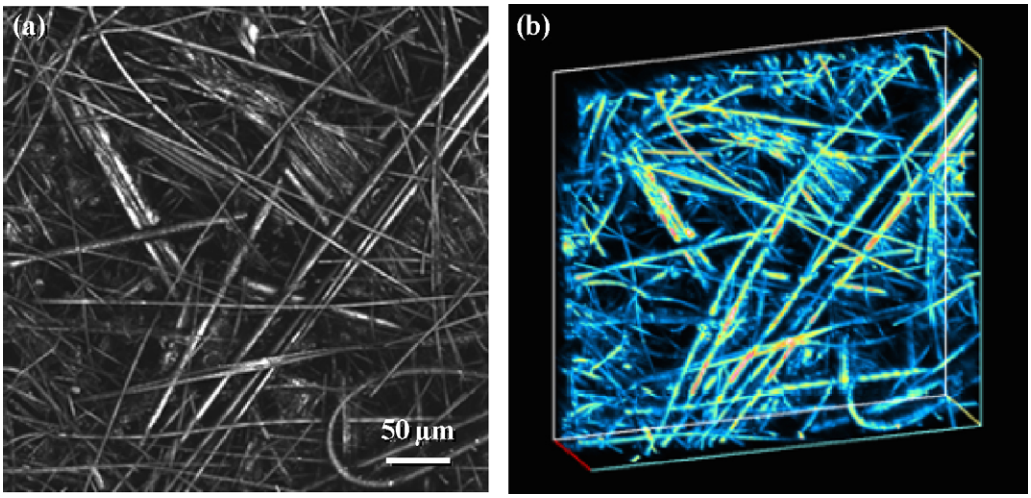

Fig. 5. CLSM images of paper-structured PtNPs catalyst (400 μm (W) × 400 μm (D) × 100 μm (H)): (a) 2D reflected image and (b) 3D fluorescent image.

catalyst (400 μm W × 400 μm D × 100 μm H). The CLSM technique revealed that the paper-structured catalyst possessed the unique porous microstructure derived from layered inorganic fiber networks. The pore size and porosity were 20–50 μm and ca. 80%, respectively, as determined by the mercury intrusion method, and corresponded roughly to reported values [27]. The chemical state of PtNPs in the paper composites exhibited the metallic Pt(0) as before (see supplementary data, Fig. S4a); however, undesirable sintering of PtNPs was recognized (Pt crystallite size: 10.0 nm), as shown in Fig. S5a.

Commercial honeycomb monolithic catalysts are generally made from cordierite ceramic components; the resulting poor thermal responsiveness is a major drawback in their practical application due to low thermal conductivity (3.0 W m^{-1} K^{-1}). In the paper-structured PtNPs catalyst, however, carbon fibers with high thermal conductivity (515 W m^{-1} K^{-1}) were successfully incorporated in a ceramic paper matrix by using our established papermaking technique, as shown in Fig. 5b. Thus the paper-structured PtNPs catalyst was expected to possess excellent thermal responsiveness by comparison with commercial honeycomb catalysts.

3.3. NO_X reduction performance

The catalytic efficiency, for reduction of NO (as a model gas of NO_X) to N_2, of the paper-structured PtNPs catalyst was compared with that of other Pt catalysts (fiber, powder and honeycomb). In each case, the amount of Pt and the occupied volume in the reactor were kept constant at 4.2 mg and 5.6 × 10^3 mm^3, respectively. Fig. 6 shows NO_X conversion and temperature profiles in the steady state. The catalytic performance of paper-structured PtNPs catalyst was superior to that of commercial Pt/Al_2O_3 powders and honeycomb monolithic catalyst. For the paper-structured paper PtNPs catalyst NO_X reduction started when the external temperature of the reactor was about 350 °C, and 80% conversion was achieved at about 420 °C. By comparison, the catalysts in powder form showed poor performance below 450 °C. Catalyst powders were blended with inorganic fibers to adjust the occupied volume of catalyst layer, and carbon fiber was far more effective than ceramic fiber, indicating the positive effect of thermal conductivity of fillers on the NO_X reduction reaction. Honeycomb monolithic catalyst displayed relatively good performance, but was inferior to paper-structured PtNPs catalyst. Random packing of PtNPs-supported carbon fibers also exhibited good performance, suggesting that PtNPs prepared by this method have higher catalytic activity than commercial powder form Pt catalysts. In any case, paper-structured PtNPs catalyst demonstrated higher NO_X conversion efficiency, although the Pt crystallite size of PtNPs in the paper composites was larger (see supplementary data, Fig. S5a). This interesting phenomenon was attributed to paper-specific structural effects, possibly due to the effective heat and mass transfer derived from the porous fiber-network structure of paper composites, as reported in our previous studies [27–32]. Internal temperatures of the reactor were proportional to the external temperatures, but higher thermal conductivity of catalyst components induced a higher internal temperature at a designated external temperature. It follows that the thermal conductivity of the catalyst matrix must be a critical factor for practical catalytic performance. Fig. 7 shows CH_4 conversion for various catalysts. The paper-structured PtNPs catalyst gave immediate CH_4 conversion at lower external temperatures by comparison with other catalyst samples. CH_4 removal is known to be achieved by exothermic CH_4 oxidation [42], leading to increase of internal temperature. Thus the relatively high internal temperature in the case of the paper-structured PtNPs catalyst (Fig. 6) may be attributable to the heat of reaction generated by CH_4 oxidation as well as to the high thermal conductivity of the carbon fiber matrix. These results indicated that the combination of PtNPs supported on carbon fibers and paper-specific microstructure is effective for the simultaneous removal of NO_X and CH_4 to purify automobile exhaust gas. Almost complete conversion of both NO_X and CH_4 was achieved at an external temperature (about 440 °C) which was 60 °C lower than for the commercial honeycomb catalyst. Carbon fibers (crystal structure) and PtNPs (oxidation state and crystallite size) in the paper composites remained almost unchanged during NO_X reduction process (see supplementary data, Figs. S4 and S5), suggesting that the paper-structured PtNPs catalyst had the practical durability to some extent. However, the surfaces of the carbon fibers used were partially oxidized as shown in C1s profile (Fig. S4b), and thus there is room for further improvement.

Thermal responsiveness is one of the requisite properties for practical applications, to ensure sufficient catalytic performance under rapid temperature changes. Fig. 8 shows NO_X conversion behavior and temperature profiles at elevated temperatures. The paper-structured PtNPs catalyst demonstrated excellent thermal response compared with the honeycomb monolithic catalyst,

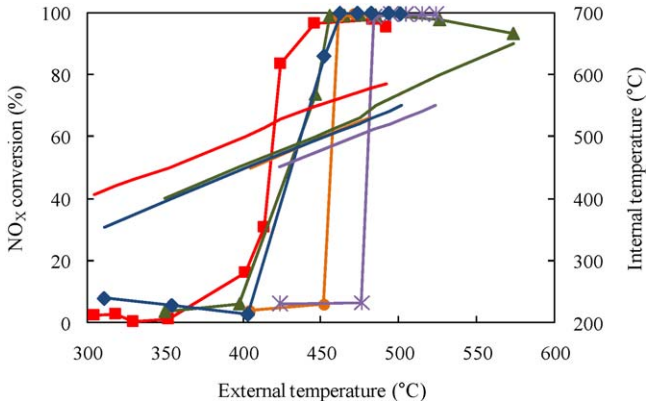

Fig. 6. NO_X conversion behavior (solid symbols) and internal temperature profiles (solid lines) of various catalysts in the steady state. Red squares: paper-structured PtNPs catalyst, green triangles: PtNPs-supported carbon fiber, orange circles: commercial Pt/Al_2O_3 powder mixed with carbon fibers, purple crosses: commercial Pt/Al_2O_3 powder mixed with ceramic fibers, blue diamonds: commercial honeycomb monolithic catalyst. (For interpretation of the references to color in this figure legend, the reader is referred to the web version of the article.)

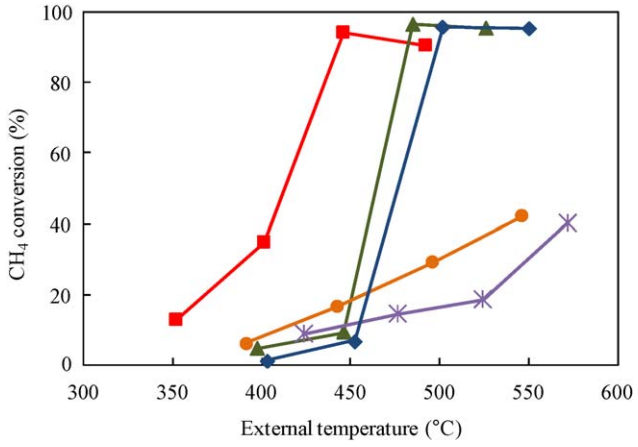

Fig. 7. CH_4 conversion behavior of various catalysts in the steady state. Red squares: paper-structured PtNPs catalyst, green triangles: PtNPs-supported carbon fiber, orange circles: commercial Pt/Al_2O_3 powder mixed with carbon fibers, purple crosses: commercial Pt/Al_2O_3 powder mixed with ceramic fibers, blue diamonds: commercial honeycomb monolithic catalyst. (For interpretation of the references to color in this figure legend, the reader is referred to the web version of the article.)

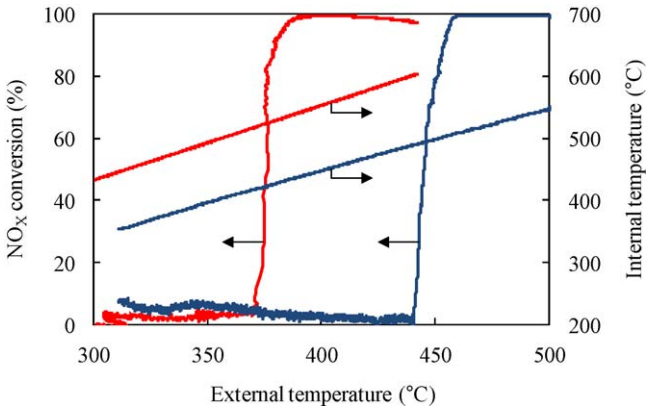

Fig. 8. NO_X conversion behavior and internal temperature profiles at elevated temperatures at 2 °C min^{-1}. Red lines: paper-structured PtNPs catalyst, blue lines: commercial honeycomb monolithic catalyst. (For interpretation of the references to color in this figure legend, the reader is referred to the web version of the article.)

indicating its advantage in a rapid start-up and with a rapid response to thermal changes. In general, ceramic honeycomb-structured catalysts composed of regularly arranged parallel channels have suffered from the lack of radial mixing of reactant gases as well as low thermal conductivity [26]. On the other hand, the paper-structured catalyst composites possess connected pore spaces derived from inorganic fiber networks (Fig. 5), which allows efficient transport of heat and reactants to the catalytic surfaces. Thus the paper-structured PtNPs catalyst, with both high thermal conductivity and unique paper structure, is expected to be a promising catalytic material for improving thermal responsiveness and gas purification efficiency.

4. Conclusion

Pt nanocatalysts were successfully synthesized on surface-activated carbon fibers with high thermal conductivity. The paper-structured matrix comprising PtNPs-supported carbon fibers and ceramic fibers was prepared by a papermaking technique. As-prepared paper-structured PtNPs catalyst display excellent performance, exemplified by NO_X reduction efficiency and rapid thermal responsiveness, by comparison with commercial Pt/Al_2O_3 catalyst powders and honeycomb monolithic catalyst. It is suggested that both highly active PtNPs scattered on a carbon fiber matrix with high thermal conductivity, and paper-structured support with fiber-network microstructure synergistically promote effective NO_X reduction. The porous, flexible and easy to handle paper-structured PtNPs catalysts are designed to fit various reactor configurations, and are thus expected to be a promising material for practical combustion exhaust gas purification.

Acknowledgements

This research was supported by a Research Fellowship for Young Scientists from the Japan Society for the Promotion of Science (H. K.) and by a Risk-Taking Fund for Technology Development from the Japan Science and Technology Agency (T. K.). The authors sincerely thank Ms. E. Tokunaga for her analytical support.

Appendix A. Supplementary data

Supplementary data associated with this article can be found, in the online version, at doi:10.1016/j.apcatb.2009.05.002.

References

[1] A. Fritz, V. Pitchon, Appl. Catal. B 13 (1997) 1–25.
[2] Q. Zhou, A. Gullitti, J. Xiao, Y. Huang, Chem. Eng. Commun. 195 (2008) 706–720.
[3] M.V. Twigg, Appl. Catal. B 70 (2007) 2–15.
[4] M. Casapu, J.-D. Grunwaldt, M. Maciejewski, F. Krumeich, A. Baiker, M. Wittrock, S. Eckhoff, Appl. Catal. B 78 (2008) 288–300.
[5] A. Kotsifa, D.I. Kondarides, X.E. Verykios, Appl. Catal. B 80 (2008) 260–270.
[6] R.D. Clayton, M.P. Harold, V. Balakotaiah, Appl. Catal. B 81 (2008) 161–181.
[7] S. Roy, M.S. Hegde, S. Sharma, N.P. Lalla, A. Marimuthu, G. Madras, Appl. Catal. B 84 (2008) 341–350.
[8] T. Nakatsuji, T. Yamaguchi, N. Sato, H. Ohno, Appl. Catal. B 85 (2008) 61–70.
[9] F.J.P. Schott, P. Balle, J. Adler, S. Kureti, Appl. Catal. B 87 (2009) 18–29.
[10] M. Shelef, R.W. McCabe, Catal. Today 62 (2000) 35–50.
[11] C. Montes de Correa, F. Córdoba, F. Bustamante, Micropororous Mesopororous Mater. 40 (2000) 149–157.
[12] J.A.Z. Pieterse, S. Booneveld, Appl. Catal. B 73 (2007) 327–335.
[13] B. White, M. Yin, A. Hall, D. Le, S. Stolbov, T. Rahman, N. Turro, S. O'Brien, Nano Lett. 6 (2006) 2095–2098.
[14] J.Y. Park, Y. Zhang, M. Grass, T. Zhang, G.A. Somorjai, Nano Lett. 8 (2008) 673–677.
[15] F. Wen, W. Zhang, G. Wei, Y. Wang, J. Zhang, M. Zhang, L. Shi, Chem. Mater. 20 (2008) 2144–2150.
[16] M. Zhao, L. Sun, R.M. Crooks, J. Am. Chem. Soc. 120 (1998) 4877–4878.
[17] S. Ivanova, V. Pitchon, Y. Zimmermann, C. Petit, Appl. Catal. A 298 (2006) 57–64.
[18] K. Mallick, M.S. Scurrell, Appl. Catal. A 253 (2003) 527–536.
[19] J.-H. Chen, J.-N. Lin, Y.-M. Kang, W.-Y. Yu, C.-N. Kuo, B.-Z. Wan, Appl. Catal. A 291 (2005) 162–169.
[20] D.M. Dotzauer, J. Dai, L. Sun, M.L. Bruening, Nano Lett. 6 (2006) 2268–2272.
[21] C. Fukuhara, H. Ohkura, Appl. Catal. A 344 (2008) 158–164.
[22] N. Semagina, M. Grasemann, N. Xanthopoulos, A. Renken, L. Kiwi-Minsker, J. Catal. 251 (2007) 213–222.
[23] H. Purnama, T. Ressler, R.E. Jentoft, H. Soerijanto, R. Schlögl, R. Schomäcker, Appl. Catal. A 259 (2004) 83–94.
[24] A. Bueno-López, D. Lozano-Castelló, I. Such-Basáñez, J.M. García-Cortés, M.J. Illán-Gómez, C. Salinas-Martínez de Lecea, Appl. Catal. B 58 (2005) 1–7.
[25] M.A. Ercoli, J.M. Zamaro, C.E. Quincoces, E.E. Miró, M.G. González, Chem. Eng. Commun. 195 (2008) 417–426.
[26] F.C. Patcas, G.I. Garrido, B. Kraushaar-Czarnetzki, Chem. Eng. Sci. 62 (2007) 3984–3990.
[27] S. Fukahori, T. Kitaoka, A. Tomoda, R. Suzuki, H. Wariishi, Appl. Catal. A 300 (2006) 155–161.
[28] S. Fukahori, H. Koga, T. Kitaoka, A. Tomoda, R. Suzuki, H. Wariishi, Appl. Catal. A 310 (2006) 138–144.
[29] S. Fukahori, H. Koga, T. Kitaoka, M. Nakamura, H. Wariishi, Int. J. Hydrogen Energy 33 (2008) 1661–1670.
[30] H. Koga, S. Fukahori, T. Kitaoka, A. Tomoda, R. Suzuki, H. Wariishi, Appl. Catal. A 309 (2006) 263–269.
[31] H. Koga, S. Fukahori, T. Kitaoka, M. Nakamura, H. Wariishi, Chem. Eng. J. 139 (2008) 408–415.
[32] H. Koga, T. Kitaoka, H. Wariishi, Chem. Commun. 43 (2008) 5616–5618.
[33] J. Garcia, H.T. Gomes, Ph. Serp, Ph. Kalck, J.L. Figueiredo, J.L. Faria, Carbon 44 (2006) 2384–2391.
[34] Y. Kojima, K.-i. Suzuki, K. Fukumoto, M. Sasaki, T. Yamamoto, Y. Kawai, H. Hayashi, Int. J. Hydrogen Energy 27 (2002) 1029–1034.
[35] S.-J. Park, J.-S. Shin, J.-W. Shim, S.-K. Ryu, J. Colloid Interface Sci. 275 (2004) 342–344.
[36] T.G. Ros, A.J. van Dillen, J.W. Geus, D.C. Koningsberger, Chem. -Eur. J. 8 (2002) 1151–1162.
[37] M.L. Toebes, J.M.P. van Heeswijk, J.H. Bitter, A.J. van Dillen, K.P. de Jong, Carbon 42 (2004) 307–315.
[38] S. Kundu, Y. Wang, W. Xia, M. Muhler, J. Phys. Chem. C 112 (2008) 16869–16878.
[39] J. Blanco, A.L. Petre, M. Yates, M.P. Martin, S. Suarez, J.A. Martin, Adv. Mater. 18 (2006) 1162–1165.
[40] M.J. Pilling, A.A. Fonseca, M.J. Cousins, K.C. Waugh, M. Surman, P. Gardner, Surf. Sci. 587 (2005) 78–87.
[41] G. Guo, F. Qin, D. Yang, C. Wang, H. Xu, S. Yang, Chem. Mater. 20 (2008) 2291–2297.
[42] J.N. Armor, Catal. Today 26 (1995) 147–158.